REPORT DOCUMENTATION PAGE

Form Approved OMB NO. 0704-0188

The public reporting burden for this collection of information is estimated to average 1 hour per response, including the time for reviewing instructions, searching existing data sources, gathering and maintaining the data needed, and completing and reviewing the collection of information. Send comments regarding this burden estimate or any other aspect of this collection of information, including suggesstions for reducing this burden, to Washington Headquarters Services, Directorate for Information Operations and Reports, 1215 Jefferson Davis Highway, Suite 1204, Arlington VA, 22202-4302. Respondents should be aware that notwithstanding any other provision of law, no person shall be subject to any oenalty for failing to comply with a collection of information if it does not display a currently valid OMB control number.
PLEASE DO NOT RETURN YOUR FORM TO THE ABOVE ADDRESS.

1. REPORT DATE (DD-MM-YYYY)	2. REPORT TYPE	3. DATES COVERED (From - To)
19-11-2007	Final Report	1-Oct-2003 - 30-Sep-2007

4. TITLE AND SUBTITLE
Final Report for ARO: "Photonic Crystal/Nano-Electronic Device Structures for Large Array Thermal Imaging"

5a. CONTRACT NUMBER
DAAD19-03-1-0370

5b. GRANT NUMBER

5c. PROGRAM ELEMENT NUMBER
611102

6. AUTHORS
Dr. Daniel C. Tsui

5d. PROJECT NUMBER

5e. TASK NUMBER

5f. WORK UNIT NUMBER

7. PERFORMING ORGANIZATION NAMES AND ADDRESSES
Princeton University
Office Of Research & Project Administration
The Trustees of Princeton University
Princeton, NJ 08544 -0036

8. PERFORMING ORGANIZATION REPORT NUMBER

9. SPONSORING/MONITORING AGENCY NAME(S) AND ADDRESS(ES)
U.S. Army Research Office
P.O. Box 12211
Research Triangle Park, NC 27709-2211

10. SPONSOR/MONITOR'S ACRONYM(S)
ARO

11. SPONSOR/MONITOR'S REPORT NUMBER(S)
45436-EL.1

12. DISTRIBUTION AVAILIBILITY STATEMENT
Approved for public release; Federal purpose rights

13. SUPPLEMENTARY NOTES
The views, opinions and/or findings contained in this report are those of the author(s) and should not contrued as an official Department of the Army position, policy or decision, unless so designated by other documentation.

14. ABSTRACT
Lattice-matched InGaAs/Inp quantum well infrared detector (QWIP) exhibits high photoconductive gain but un-adjustable detection wavelength because of its fixed barrier height. The use of InxGa1-xAsyP1-y (InGaAsP) as the barrier material is superior to that of InP with regard to the flexibility of operating wavelength. In this letter we investigate the application of InGaAsP material in the long–wavelength infrared detection. We report a broadband quantum well InGaAs/InGaAsP detector covering 8-14 m. The excellent agreement between the observed responsivity spectrum and the calculated one is achieved indicating the validness of our design model. In order to determine the usefulness of InGaAsP in long-wavelength detection,

15. SUBJECT TERMS
Voltage-tunable, InGaAs barrier, InGaAs/InGaAsP, Superlattice, Photocurrent

16. SECURITY CLASSIFICATION OF:			17. LIMITATION OF ABSTRACT	15. NUMBER OF PAGES	19a. NAME OF RESPONSIBLE PERSON
a. REPORT	b. ABSTRACT	c. THIS PAGE			Daniel Tsui
U	U	U	SAR		19b. TELEPHONE NUMBER: 609-258-4621

Report Title

Final Report for ARO: "Photonic Crystal/Nano-Electronic Device Structures for Large Array Thermal Imaging"

ABSTRACT

Lattice-matched InGaAs/Inp quantum well infrared detector (QWIP) exhibits high photoconductive gain but un-adjustable detection wavelength because of its fixed barrier height. The use of InxGa1-xAsyP1-y (InGaAsP) as the barrier material is superior to that of InP with regard to the flexibility of operating wavelength. In this letter we investigate the application of InGaAsP material in the long–wavelength infrared detection. We report a broadband quantum well InGaAs/InGaAsP detector covering 8-14 m. The excellent agreement between the observed responsivity spectrum and the calculated one is achieved indicating the validness of our design model. In order to determine the usefulness of InGaAsP in long-wavelength detection, we also design a GaAs/AlGaAs quantum well detector with similar spectrum and compare its performance with that of the InGaAs/InGaAsP detector. The dark current noise measurement indicates that the gain in InGaAsP is 4.6 times larger than that of AlGaAs, showing that InGaAsP is a good candidate for long-wavelength high-speed infrared detection.

List of papers submitted or published that acknowledge ARO support during this reporting period. List the papers, including journal references, in the following categories:

(a) Papers published in peer-reviewed journals (N/A for none)

1. J. Li, K.K. Choi, J.F. Klem, J.L. Reno, D.C. Tsui, “High gain, broadband InGaAs/InGaAsP quantum well infrared photodetector”, submitted to Applied Physics Letter.
2. J. Li, K.K. Choi, D.C. Tsui, “Voltage-tunable four-color quantum well infrared photodetector”, Applied Physics Letters, 86 (21), 211114 (2005).
3. K.K. Choi, C. Monroy, A. Goldberg, G. Dang, M. Jhabvala, A. La, T. Tamir, K.M. Leung, A. Majumdar, J. Li, D.C. Tsui, “Designs and applications of corrugated QWIPs", Inf. Phys. & Tech., In press.

Number of Papers published in peer-reviewed journals: 3.00

(b) Papers published in non-peer-reviewed journals or in conference proceedings (N/A for none)

Number of Papers published in non peer-reviewed journals: 0.00

(c) Presentations

Number of Presentations: 0.00

Non Peer-Reviewed Conference Proceeding publications (other than abstracts):

1. J. Li, K.K. Choi, J.F. Klem, J.L. Reno, D.C. Tsui, “Study of a broadband high-gain InGaAs/InGaAsP quantum-well infrared photodetector”, Applied Physics Society March Meeting, Baltimore, MD, USA, March 13 - 17, 2006.
2. K.K. Choi, C. Monroy, T. Tamir, M. Leung, J. Li, D. C. Tsui, “Developing a voltage tunable two-color corrugated QWIP focal plane array”, Applied Physics Society March Meeting, Baltimore, MD, USA, March 13 - 17, 2006.
3. J. Li, K.K. Choi, D.C. Tsui, “Voltage tunable four-color infrared detector using semiconductor superlattices”, SPIE’s Optics & Photonics 2005, San Diego, California, USA, July 31-August 4, 2005, 588102-1.

Number of Non Peer-Reviewed Conference Proceeding publications (other than abstracts): 3

Peer-Reviewed Conference Proceeding publications (other than abstracts):

Number of Peer-Reviewed Conference Proceeding publications (other than abstracts): 0

(d) Manuscripts

Number of Manuscripts: 0.00

Number of Inventions:

Graduate Students

NAME	PERCENT_SUPPORTED
FTE Equivalent:	
Total Number:	

Names of Post Doctorates

NAME	PERCENT_SUPPORTED
Gabor Csathy	0.25
Jian Huang	1.00
Amlan Majumdar	1.00
Hwayong Noh	1.00
Tao Zhou	1.00
Jinjin Li	1.00
FTE Equivalent:	**5.25**
Total Number:	**6**

Names of Faculty Supported

NAME	PERCENT_SUPPORTED	National Academy Member
Daniel C. Tsui	0.24	Yes
FTE Equivalent:	**0.24**	
Total Number:	**1**	

Names of Under Graduate students supported

NAME	PERCENT_SUPPORTED
FTE Equivalent:	
Total Number:	

Student Metrics

This section only applies to graduating undergraduates supported by this agreement in this reporting period

The number of undergraduates funded by this agreement who graduated during this period:	0.00
The number of undergraduates funded by this agreement who graduated during this period with a degree in science, mathematics, engineering, or technology fields:.....	0.00
The number of undergraduates funded by your agreement who graduated during this period and will continue to pursue a graduate or Ph.D. degree in science, mathematics, engineering, or technology fields:.....	0.00
Number of graduating undergraduates who achieved a 3.5 GPA to 4.0 (4.0 max scale):	0.00
Number of graduating undergraduates funded by a DoD funded Center of Excellence grant for Education, Research and Engineering:	0.00
The number of undergraduates funded by your agreement who graduated during this period and intend to work for the Department of Defense	0.00
The number of undergraduates funded by your agreement who graduated during this period and will receive scholarships or fellowships for further studies in science, mathematics, engineering or technology fields:	0.00

Names of Personnel receiving masters degrees

NAME

Total Number:

Names of personnel receiving PHDs

NAME

Total Number:

Names of other research staff

NAME PERCENT_SUPPORTED

FTE Equivalent:

Total Number:

Sub Contractors (DD882)

Inventions (DD882)

Final Report for
ARO: "Photonic Crystal/ Nano-Electronic Device Structures for Large Array Thermal Imaging"

Period: October 1, 2003 – September 30, 2007

Professor Daniel Tsui
Department of Electrical Engineering
Princeton University
(Account #: 170-6429)
November 19, 2007

Journal Publications during Reporting Period

1. J. Li, K.K. Choi, J.F. Klem, J.L. Reno, D.C. Tsui, "High gain, broadband InGaAs/InGaAsP quantum well infrared photodetector", submitted to Applied Physics Letter.
2. J. Li, K.K. Choi, D.C. Tsui, "Voltage-tunable four-color quantum well infrared photodetector", Applied Physics Letters, 86 (21), 211114 (2005).
3. K.K. Choi, C. Monroy, A. Goldberg, G. Dang, M. Jhabvala, A. La, T. Tamir, K.M. Leung, A. Majumdar, J. Li, D.C. Tsui, "Designs and applications of corrugated QWIPs", Inf. Phys. & Tech., In press.

Conference Publications

1. J. Li, K.K. Choi, J.F. Klem, J.L. Reno, D.C. Tsui, "Study of a broadband high-gain InGaAs/InGaAsP quantum-well infrared photodetector", Applied Physics Society March Meeting, Baltimore, MD, USA, March 13 - 17, 2006.
2. K.K. Choi, C. Monroy, T. Tamir, M. Leung, J. Li, D. C. Tsui, "Developing a voltage tunable two-color corrugated QWIP focal plane array", Applied Physics Society March Meeting, Baltimore, MD, USA, March 13 - 17, 2006.
3. J. Li, K.K. Choi, D.C. Tsui, "Voltage tunable four-color infrared detector using semiconductor superlattices", SPIE's Optics & Photonics 2005, San Diego, California, USA, July 31-August 4, 2005, 588102-1.

Post-Docs, Graduate Students, Faculty Supported

<u>Professional Researchers/Postdoctoral Associates</u>
Csathy, Gabor A.
Feb 2006 – May 2006: 25%

Huang, Jian
Oct 2004 – Dec 2004: 100%

Li, Jinjin:
April 2004 – May 2004: 100%
March 2005 – Jan 2006: 100%

Majumdar, Amlan:
Nov 2003 – Jan 2004: 100%

Noh, Hwayong:
Oct 2003 – Jan 2004: 100%

Zhou, Tao:
Jun 2004 – Aug 2004: 100%

Graduate students
NONE

Undergraduate students
NONE

Faculty
Tsui, Daniel C:
Summer 2005: 18%
Summer 2006: 30%

Inventions and Patents
None

Honors and Awards
None

Keywords
Voltage-tunable, InGaAs barrier, InGaAs/InGaAsP, Superlattice, Photocurrent

Scientific Progress and Accomplishments

Voltage-tunable four-color QWIPs
Voltage-tunable multi-color QWIPs are highly desirable in many important applications. The existing designs suffer from limited range of tunability and substantial spectral cross-talk [1-6]. We therefore solved these problems and developed the world's first semiconductor four-color QWIP which demonstrated four distinct narrowband peaks without spectral cross-talk in a single device.

The layer structure and the schematic energy-band diagram of the detector are shown in Fig. 1. The detector consists of two stacks of superlattice (SL) materials that are separated by a middle contact layer. Each material is designed to detect two specific wavelengths, one middle wavelength (MW) and one long wavelength (LW), tunable by the bias polarity. Four-color

detection is achieved by applying different combinations of top and bottom biases relative to the common middle contact.

A 45° edge-coupled detector with area of 1200 × 700 μm^2 was fabricated. The spectral responsivity R of the detector at T = 10 K at different biases V_b is shown in Fig. 2. As expected, four narrowband peaks centered at 4.5 μm, 5.3 μm, 8.3 μm, and 10.4 μm with corresponding spectral width $\Delta\lambda$ of 0.58 μm, 0.71 μm, 0.83 μm, and 1.01 μm are observed.

Spectral cross-talk, which refers to the presence of the middle wavelength (MW) peak at both positive and negative biases, is a significant challenge to the design of voltage-tunable multi-color detectors. Our detector has solved this problem successfully, as illustrated in Fig. 2. The origin of the cross-talk is the built-in field of the blocking barrier connecting the two SLs. To prevent the cross-talk, we need to eliminate the MW response from the LW detection under negative bias. Towards this end, two methods are applied. First, instead of the simply graded barrier, a step-graded-step barrier is applied as the blocking barrier. The step next to the MW SL can raise the effective height of the blocking barrier under negative bias, hence preventing the transfer of MW electrons into the barrier. Consequently, spectral cross-talk is eliminated since only LW photocurrent is presented at negative bias. Second, a narrow miniband of MW SL is applied, which can help to prevent the formation of the high energy electrons and therefore eliminate the MW response at the negative bias.

We compare the measured spectral responses with the calculated ones in Fig. 3 and clearly observe the good agreement between them. The calculated responsivity was done using the material parameters given by Shi *et al* [7]. With the conventional conduction band offset of ΔE = $0.6\Delta E_g$, where ΔE_g is the bandgap difference between AlGaAs and GaAs, the calculated spectra of the two MW bands, namely the 4.5 and 5.3 μm bands, match the experimental data well. However, we found that ΔE needs to be increased to $0.82\Delta E_g$ to match the 8.3 and 10.4 μm detection peaks. In addition to ΔE, another parameter in the fitting is the standard deviation of each individual transition caused by inhomogeneous broadening, which is found to be 10, 10, 6.5, and 5 meV for the 4.5, 5.3, 8.3 and 10.4 μm peaks, respectively.

Fig. 4 plots the dark current density J_d at different temperatures along with the window current density J_w at 10 K. J_w is generated by 300 K background radiation and measured by F/1.2 optics. The device is under background-limited infrared performance (BLIP) below 100 K at V_b = 1.5 V for 4.5 μm detection, 80 K at V_b = 1.5 V for 5.3 μm detection, 60 K at V_b = -1.2 V for 8.3 μm detection, and 50 K at V_b = -1.1 V for 10.4 μm detection. These BLIP temperatures are comparable to those of single-color detectors optimized in the respective bands.

In conclusion, we have successfully demonstrated a voltage-tunable four-color infrared photodetector that detects a different single color at each bias combination without spectral cross-talk. The detection spectrum does not change with temperature, and the background limited temperatures are satisfactory. The detection peaks can be randomly selected between 3 μm and 20 μm, and each peak can vary from narrow band to broadband. The present detector design thus improves the QWIP technology in multi-color detection.

On the other hand, for this developed four-color detector, we note that the LW responses are approximately one order of magnitude below those of the normal designs. The small LW R is due to the low mobility of the LW photoelectrons. When the potential drop per SL period is larger than the M_2 width of each SL, the miniband states become localized, and the photoelectrons are transported across the SLs through sequential tunneling, resulting in a much lower mobility. This affects all four bands; however it reduces the LW R more significantly, because the M_2 miniband of LW is deeper below the SL barrier and consequently the tunneling is much weaker. The smaller R necessitates a longer integration time in infrared detection. Nevertheless, the sensitivity of the detector, which depends on the photocurrent to dark current ratio, is unaffected since the thermal dark current is reduced proportionally due to the small tunneling rate.

New structures are designed to improve the LW responsivity. In the new designs, the LW SL, which is with high barrier, is replaced by the low barrier, weakly-coupled multiple quantum well (MQW) structure. However, because of the lower barrier of the MQW, MW photocurrent may exist during the LW operation. To solve this problem, it is necessary to increase the electron density in the spacer layer (n^+ hot-electron reservoir) and the length of the spacer layer. Numerical simulations are carried out to study the electron relaxation process in the spacer layer to provide suitable design parameters to the spacer layer. The final layer structure of the detector is shown in Fig. 5. Furthermore, to better understand the electron relaxation process in the spacer layer, we made two designs, which are identical except the different electron doping densities in the spacer layer. With these two designs, we potentially can derive the energy relaxation rate of the electron. The solution of this problem will give guidelines for the future detector design with regard to the elimination of the spectral crosstalk.

Unfortunately the experimental results on these two new designs are not as expected. We believe some of the problems result from the growth of the material. The experimentally observed spectrum is shifted from the calculated one, which clearly is due to the mismatch between the theoretical and the practical fitting parameters. Such mismatch could be caused by the inaccuracy of the calibration of the MBE machine. Our future work will include: re-growth and re-characterizing of the new detector structures.

<u>High gain, broadband InGaAS/InGaAsP QWIPs</u>

High speed infrared detection is highly important and desirable for tracking fast moving objects. For high speed application, the integration time of the system readout circuit is too short to collect enough signals. In this case, the constant readout noise dominates. Consequently in order to improve the signal to noise ratio of the detection, a larger photocurrent is desirable. To increase the photocurrent of QWIPs, one needs to obtain a large quantum efficiency η, a high photoconductive gain g, and a large absorption spectral width Γ. While η is related to the light coupling scheme and has no much space to be improved, g is determined by material properties, and Γ depends on the design structure. We therefore manipulated with g and Γ and devised a material structure that achieves high g and large Γ simultaneously. The developed QWIP is suitable for high-speed applications.

Compared to conventional GaAs/AlGaAs QWIPs, lattice-matched InGaAs/InP QWIPs exhibit high photoconductive gain [8-14] but nonadjustable detection wavelength because of their fixed

barrier height. The use of $In_xGa_{1-x}As_yP_{1-y}$ (InGaAsP) as the barrier material is superior to that of InP with regard to flexibility of the operating wavelength. Therefore, in this work, we presented the design and fabrication of a QWIP with InGaAsP barriers to assess its capability in providing a large gain. For the broadband detection, there are many QW structures [15-20]. Among them, the strongly-coupled SL design can provide the most desirable detector characteristics. We therefore employed an InGaAs/InP SL as the well region in our QWIP.

By applying the SL structure for broadband response and InGaAsP barriers for high gain, our goal is to obtain a large photocurrent. To ascertain the advantages of the InGaAs/InGaAsP QWIP over GaAs/AlGaAs QWIP, we also fabricated a GaAs/AlGaAs QWIP with very similar spectral coverage for a quantitative comparison.

The layer structure of the InGaAs/InGaAsP detector is shown in Fig. 6 (a). The detector consists of 19 SLs, which are separated by $In_{0.8}Ga_{0.2}As_{0.43}P_{0.57}$ barriers. The active material is sandwiched between top and bottom contact layers. Similarly, the GaAs/AlGaAs detector contains 8 periods of SLs separated by $Al_{0.17}Ga_{0.83}As$ barriers, as shown in Fig. 6 (b).

45° edge-coupled detectors with area of 200 × 200 μm^2 were fabricated. Figure 7 (a) and (b) plot the spectral responsivity R of the InGaAs/InGaAsP detector and the GaAs/AlGaAs detector for different electric fields F_b (F_b is defined by the applied bias divided by SL period N and is expressed in unit of volts/period). Both detectors show broadband spectral response. Under F_b = −44.7 mV/period, the R_{peak} for the InGaAs/InGaAsP detector is about 2.8 times larger than that of the GaAs/AlGaAs detector. Therefore, the InGaAsP material is able to provide a larger responsivity. We also compare the measured spectral responses with the calculated ones for the two detectors in Fig. 7 (a) and (b) and observe the good agreement between them.

The gain g of a QWIP is the most important parameter for a high speed detector. The dark current noise measurements were carried out to obtain the gain of the two detectors. The measured noise gain represents the average gain of the photoelectrons in excited states. The values of g for both detectors are shown in Fig. 8 (a). We observe that the InGaAs/InGaAsP detector, despite having a larger N, generally exhibits a higher gain. It is known that g is inversely proportional to N for a QWIP [21, 22]. To account for the different N, we scale the measured g to g_1, which represents the gain when N = 1, for both detectors using the formula $g_1 = gN$, and plot g_1 in Fig. 8 (b). The value of g_1 reflects the intrinsic properties of the materials. It shows that the InGaAs/InGaAsP detector possesses a significantly larger g_1 than the GaAs/AlGaAs detector. At F_b = −40 mV/period, g_1 is 4.6 times larger, illustrating the advantage of the detector in providing a large gain. Since the difference in g_1 is more than the difference in R, we conclude that the larger R of the InGaAs/InGaAsP detector is due to its larger gain.

Figure 9 compares the dark current density J_d and the window current density J_w for the two detectors. The InGaAs/InGaAsP detector is under BLIP below 30 K for $-55 \le F_b \le 65$ mV/period, corresponding to $-1 \le V_b \le 1.2$ V. Compared with that of the GaAs/AlGaAs detector, J_w of the InGaAs/InGaAsP detector at the positive bias is approximately three times larger, which is consistent with the ac responsivity measurement. Since the broadband GaAs/AlGaAs QWIP has 3 times higher photocurrent than a narrow band one, we conclude that the InGaAs/InGaAsP detector can provide up to an order of magnitude larger broadband

photocurrent than a regular QWIP, and thus is able to improve the detection speed. Therefore, the advantage of our approach for high speed infrared detection is convincingly verified.

In conclusion, we successfully developed a high gain, broadband InGaAs/InGaAsP QWIP which is suitable for high speed infrared detection. We also confirmed the capability of InGaAsP in providing a large gain.

References

[1] M. Z. Tidrow, X. Jiang, S. S. Li, and K. Bacher, Appl. Phys. Lett. 74, 1335, (1999).
[2] A. Majumdar, K. K. Choi, J. L. Reno, and D. C. Tsui, Appl. Phys. Lett. 80, 707 (2002).
[3] A. Majumdar, K. K. Choi, J. L. Reno, and D. C. Tsui, Appl. Phys. Lett. 83, 5130 (2003).
[4] M. Z. Tidrow, K. K. Choi, C. Y. Lee, W. H. Chang, F. J. Towner, and J. S. Ahearn, Appl. Phys. Letter. 64, 1268 (1993)
[5] Jung-chi Chiang and Sheng S. Li, M. Z. Tidrow, P. Ho, M. Tsai, and C. P. Lee, Appl. Phys. Lett. 69, 2412 (1996)
[6] K. Kheng, M. Ramsteiner, H. Schneider, J. D. Ralston, F. Fuchs, and P. Koidl, Appl. Phys. Lett. 61, 666 (1992).
[7] J. J. Shi and E. M. Goldys, IEEE trans. Electron Devices 46, 83 (1999).
[8] S. D. Gunapala, B. F. Levine, D. Ritter, R. Hamm, and M. B. Panish, Appl. Phys. Lett. 58, 2024 (1991).
[9] S. D. Gunapala, B. F. Levine, D. Ritter, R. Hamm, and M. B. Panish, Appl. Phys. Lett. 60, 636 (1992).
[10] O. O. Cellek, S. Ozer, and C. Besikci, IEEE J. Quantum Electron. 41, 980 (2005).
[11] C. Jelen, S. Slivken, T. David, M. Razeghi, and G. J. Brown, IEEE J. Quantum Electron. 34, 1124 (1998).
[12] H. C. Liu, C. Song, E. Dupont, P. Poole, P. H. Wilson, B. J. Robinson, and D. A. Thompson, Eletron. Lett. 35, 2055 (1999).
[13] J. Jiang, C. Jelen, and M. Razeghi, IEEE Photon. Technol. Lett. 14, 372 (2002).
[14] B. Aslan, H. C. Liu, A. Bezinger, P. J. Poole, M. Buchanan, R. Rehm, and H. Schneider, Semicond. Sci. Technol. 19, 442, (2004)
[15] B. F. Levine, G. Hasnain, C. G. Bethea, and N. Chand, Appl. Phys. Lett. 54, 2704 (1989).
[16] S. D. Gunapala, B. F. Levine, and N. Chand, J. Appl. Phys. 70, 305 (1991).
[17] S. V. Bandara, S. D. Gunapala, J. K. Liu, E. M. Luong, J. M. Mumolo, W. Hong, D. K. Sengupta, and M. J. McKelvey, Appl. Phys. Lett. 72, 2427 (1998).
[18] J. H. Lee, S. S. Li, M. Z. Tidrow, W. K. Liu, and K. Bacher, Appl. Phys. Lett. 75, 3207 (1999).
[19] J. Chu, S. S. Li, and A. Singh, IEEE J. Quantum Electron. 35, 312 (1999).
[20] A. R. Ellis, Amlan Majumdar, K. K. Choi, J. L. Reno, and D. C. Tsui, Appl. Phys. Lett. 84, 5127 (2004).
[21] E. Rosencher, F. Luc, P. Bois, J. Nagle, and Y. Cordier, Appl. Phys. Lett. 63, 3312 (1993).
[22] K. K. Choi, *The Physics of Quantum Well Infrared Photodetectors* (World Scientific, New Jersey, 1997).

Figures

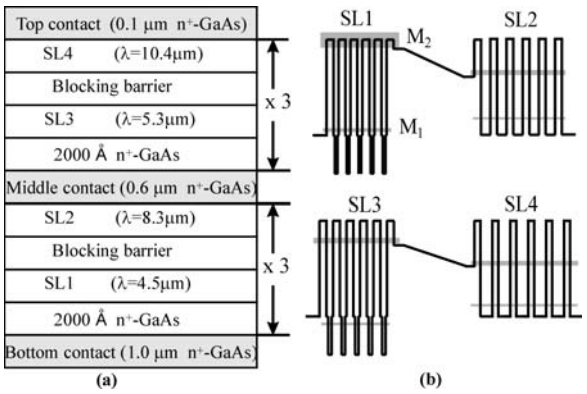

Fig. 1. (a) Material layer structure and (b) energy-band diagram of the four-color QWIP.

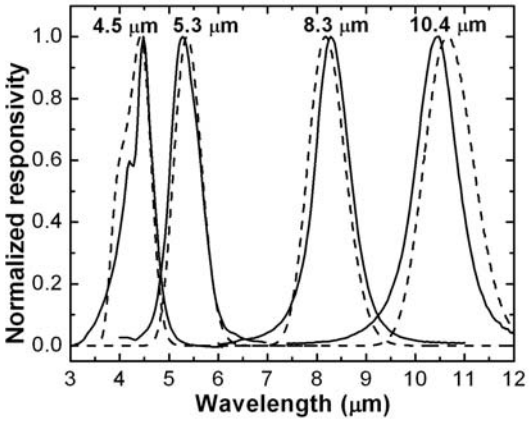

Fig. 3. Measured (solid curves) and the calculated (dashed curves) photoresponse spectra of the four-color QWIP.

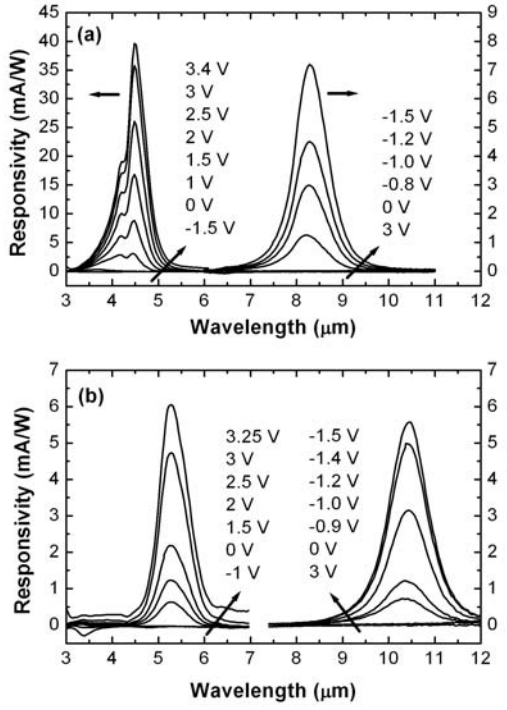

Fig. 2. Spectral responsivity R of (a) the SL1/SL2 stack and (b) the SL3/SL4 stack of 45° edge-coupled four-color QWIP at 10 K for different V_b.

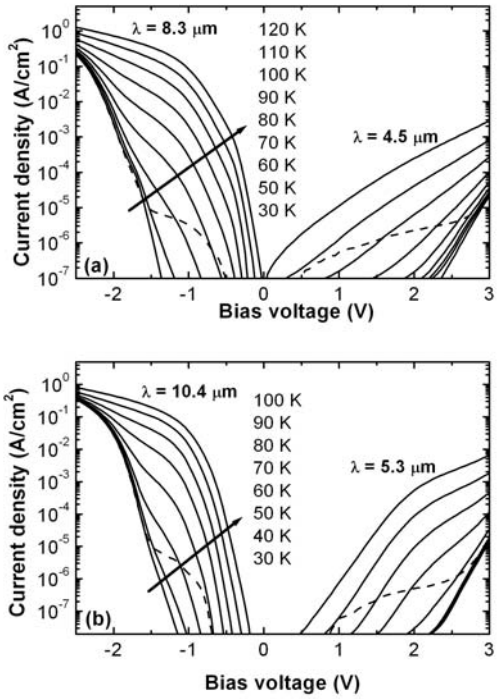

Fig. 4 Dark current density J_d (solid lines) and background photocurrent density J_w (dashed line) of (a) the SL1/SL2 stack and (b) the SL3/SL4 stack for the four-color QWIP.

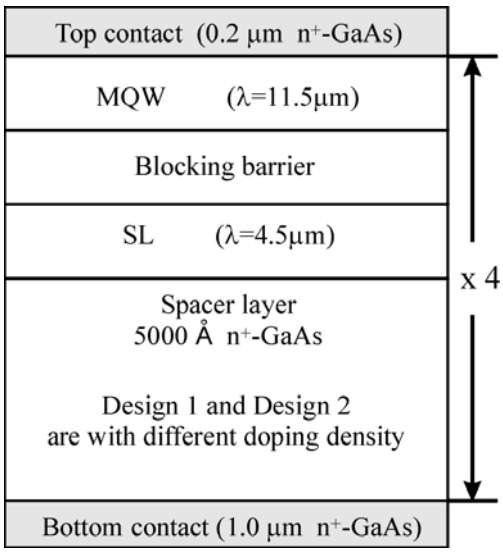

Fig. 5 Material layer structure of the two new designs of the multicolor detector.

(a)

	0.1 μm n^+-$In_{0.53}Ga_{0.47}As$	
SL	27 Å InP / 94 Å $In_{0.53}Ga_{0.47}As$	×4
Barrier	940 Å $In_{0.8}Ga_{0.2}As_{0.43}P_{0.57}$	× 19
	2.0 μm n^+-$In_{0.53}Ga_{0.47}As$	

(b)

	0.2 μm n^+-GaAs	
	50 Å $Al_{0.17}Ga_{0.83}As$	
SL	75 Å GaAs / 30 Å $Al_{0.23}Ga_{0.77}As$ / 70 Å GaAs / 30 Å $Al_{0.23}Ga_{0.77}As$	×3
	75 Å GaAs / 30 Å $Al_{0.23}Ga_{0.77}As$ / 70 Å GaAs	× 7
Barrier	600 Å $Al_{0.17}Ga_{0.83}As$	
	75 Å GaAs / 30 Å $Al_{0.23}Ga_{0.77}As$ / 70 Å GaAs / 30 Å $Al_{0.23}Ga_{0.77}As$	×3
	75 Å GaAs / 30 Å $Al_{0.23}Ga_{0.77}As$ / 70 Å GaAs	
	50 Å $Al_{0.17}Ga_{0.83}As$	
	2.5 μm n^+-GaAs	

Fig. 6 Material layer structure of (a) the InGaAs/InGaAsP detector and (b) the GaAs/AlGaAs detector.

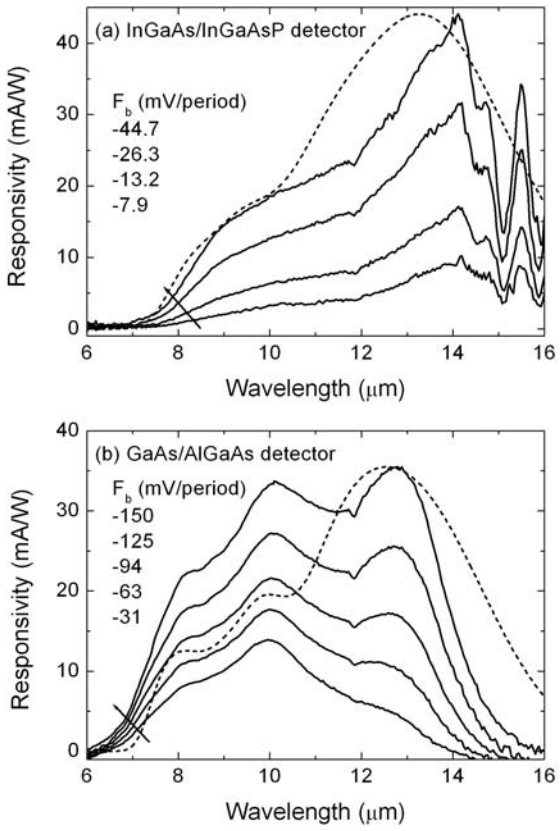

Fig. 7 Measured (solid lines) and calculated (dashed line) spectral responsivity R of (a) the InGaAs/InGaAsP detector and (b) the GaAs/AlGaAs detector at 10 K for different applied electric field F_b.

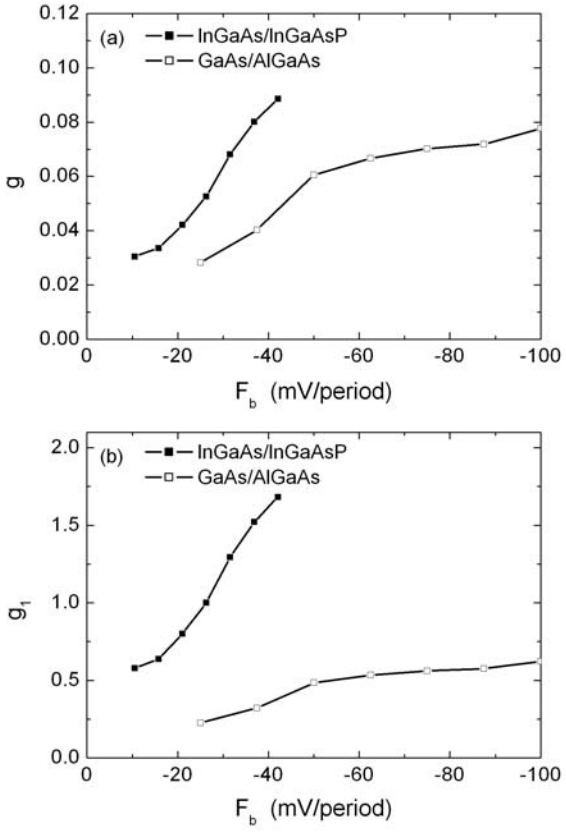

Fig. 8 Comparison of (a) noise gain g and (b) effective noise gain g_1 between the InGaAs/InGaAsP detector and the GaAs/AlGaAs detector.

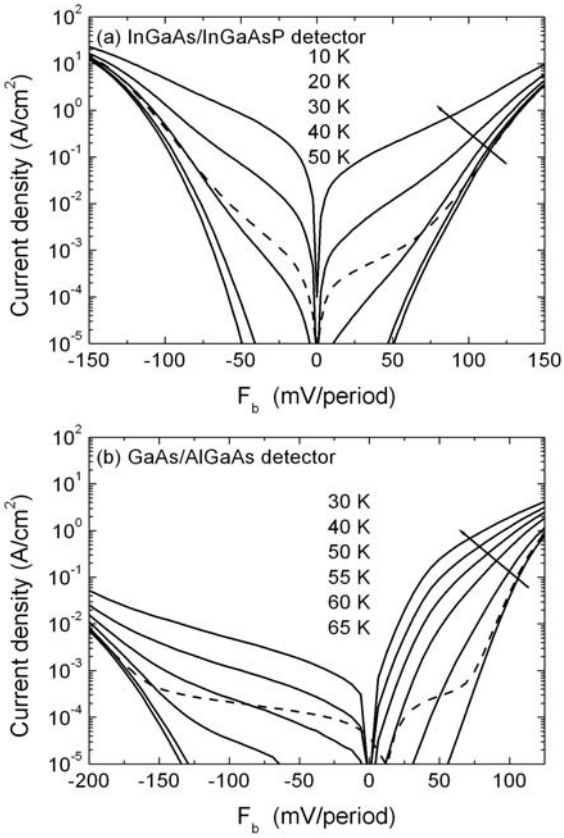

Fig. 9 Dark current density J_d (solid lines) and background photocurrent density J_w (dashed line) of (a) the InGaAs/InGaAsP detector and (b) the GaAs/AlGaAs detector.